



Enhanced dielectric properties of graphene and conjugated terpolymer-blended polyvinylidene difluoride

NARAYANASAMY KAVITHA¹, AYYAVU CHANDRAMOHAN², KRISHNAN SRINIVASAN¹, PEETHAMBARAM PRABUKANTHAN³ and KANNAIYAN DINAKARAN^{1,*} 

¹Department of Chemistry, Thiruvalluvar University, Vellore 632115, India

²Department of Chemical Engineering, Sri Sivasubramaniya Nadar College of Engineering, Chennai 603110, India

³Department of Chemistry, Muthurangam Government Arts College, Vellore 632002, India

*Author for correspondence (kdinakaran.tvu@gmail.com; kdinakaran@tvu.edu.in)

MS received 29 August 2022; accepted 26 December 2022

Abstract. In this study, electrically conductive composites of ethylenedioxythiophene-based terpolymer (PETCH), polyvinylidene difluoride (PVDF) and graphene nanosheets (GNS) have been prepared by compression molding and characterized. A new conjugated PETCH polymer was synthesized and its chemical structure has been confirmed by Fourier transform infrared and ¹H-NMR spectroscopy. The varying weight percentages of (1, 3 and 5%) GNS and 10 wt% PETCH dispersed PVDF nanocomposites were prepared and characterized using X-ray diffraction, thermogravimetric analysis, scanning electron microscopy and energy-dispersive X-ray spectroscopy (EDX) analysis. The thermal studies indicated that the decomposition occurred at a temperature around 220°C, and 480°C corresponds to the PETCH and PVDF/PETCH/GNS (1, 3 and 5%), respectively. The EDX spectrum of neat PETCH polymer and their composites of PVDF/PETCH/GNS (1, 3 and 5%) result clearly shows the presence of all elements such as, C, O, S, F and Cl with an atomic weight percentage. The PVDF/PETCH/5% GNS has a dielectric constant value of 3.9 at 1 MHz and the conductivity of this polymer composites value is found to be 5.8×10^{-6} S cm⁻¹ at 1 MHz, respectively. Results obtained from the dielectric studies indicated that the GNS and terpolymer-dispersed PVDF composites exhibit good interfacial adhesion as evidenced from conductive behaviours.

Keywords. Conductive polymer composites; terpolymer; polyvinylidene difluoride; graphene nanosheets; dielectric constant; conductivity.

1. Introduction

The advancements in modern technology and electronic gadgets require new type of conductive polymer composites with improved electrical conductivity, thermal and chemical properties to replace metal-based conductors and/or to protect the gadgets from electromagnetic radiation interference [1–3]. The intrinsic properties of conductive polymer composites, such as conductivity, biodegradability, high strength, and recyclability, enable them to be applied in several novel applications, including fuel cells, electromagnetic interference (EMI) shielding materials, drug transfer neural probes, bio-actuators, antennas etc. [4, 5]. The most promising EMI shielding materials are those with conductive polymer composite matrix and/or combined with conductive fillers [1, 6–9].

The most significant conductive polymers studied in EMI shielding applications are polypyrrole (PPy) [10], polyacetylene (PA) [11], polyaniline (PANI) [12, 13], polyvinylidene fluoride (PVDF) [14] and polyethylene dioxythiophene (PEDOT) [15], which have inherent

electrical conductivity. Among the conducting polymers, PVDF has been the subject of extensive research due to its exceptional pyro- and piezoelectric capabilities, large intrinsic polarization, good flexibility, low cost, ease of processing and lightweight. In addition, due to its superior characteristics and high permittivity, PVDF has been used in high-charge storage capacitors, micro-electronic devices, transducers, sensors, memory devices, actuators, and EMI shielding materials [16–24]. The polymer-based EMI shielding materials find application as a coating material for the medical and broadcasting equipment, which can prevent the interference of EM radiation and thereby reduces the noise and in-turn enhance the performance of said equipment. PVDF nanocomposite exhibits tunable ferroelectric and piezoelectric properties owing to its semi-crystalline nature that can be tailored through the processing conditions, which have an effect on the crystallization behaviour [25, 26]. The dielectric properties of PVDF need to be enhanced to meet future requirements in electronics and EMI shielding efficiency applications, and hence in the present work, it has been attempted to prepare PVDF

composites having increased dielectric properties by the incorporation of conjugated terpolymer containing PEDOT and graphene nanosheets (GNSs).

The polythiophene derivatives have drawn a lot of attention in recent years [27, 28], particularly PEDOT, which is made of ethylenedioxythiophene (EDOT) monomers, has attracted a great deal of attention due to its good electrochemical characteristics, affordability, good transparency and cathodic electrochromic behaviour [29, 30]. On the other hand, in order to develop the characteristics of the matrix made of conducting polymers, an immense effort has been made to add numerous types of carbon-based fillers such as carbon nanotubes (CNT) [31, 32], GNS [33], graphene oxide (GO) [34], graphene nanofibres (GNF) [35]. Among them, due to the outstanding charge-transfer capabilities, substantial specific surface area and superior mechanical attributes, the widely spread use of two-dimensional (2D) material known as graphene nanosheet has become a research hotspot with potential applications [36, 37].

For instance, Gebrekrsto *et al* [38] studied the mechanism of formation of the electroactive β -phase and the effects of nanofillers on the dielectric properties of PVDF membrane. Ahmed *et al* [39] reported the electromagnetic shielding efficiency (SE) of ~ 16 and 22 dB for PVDF/graphene and PVDF/graphene/nickel ferrite, respectively. A multi-component composite of PVDF incorporated with CNT, graphene and NiCo particles reported to have an outstanding EMI shielding efficiency of 63.3 dB and an electrical conductivity of 9.12 S cm^{-1} [40]. A composite nanomaterial of PVDF blended with PEDOT-block-PEG block copolymer, GNSs and CuO nanoparticles exhibited a dielectric constant of 34 and dielectric loss values of 9.2 at the lower region of frequency (100 Hz and at 150°C). The composite was also found to have an electromagnetic radiation shielding of 17 dB at Ku-band frequency region [41].

In the present work, we have developed highly conductive nanocomposites by GNS and ethylenedioxythiophene-based terpolymer-dispersed polyvinylidene difluoride composites [PVDF/PETCH (10%)/GNS (1, 3, 5%)]. It is to be noted that conjugated terpolymer has not been studied with PVDF for dielectric applications so far, we anticipate that the compatibility and interfacial adhesive nature will play a crucial role in the transport of electrons across the boundary. Data obtained from different studies, such as Fourier transform infrared (FT-IR), $^1\text{H-NMR}$, X-ray powder diffraction (XRD), scanning electron microscopy (SEM), energy-dispersive X-ray spectroscopy (EDX), thermogravimetric analysis, thermogravimetric-differential scanning calorimetry (TG-DSC) and dielectric studies, suggest that the GNS and thiophene-based terpolymer-dispersed PVDF composites, prepared in the present work, own good morphological, thermal and dielectric properties suitable to be used in EMI shielding materials.

2. Experimental

2.1 Materials

All the reagents are derived from commercial vendors' and used as received. 3,4-Ethylene dioxythiophene (EDOT) was purchased from Sigma-Aldrich. 4-Chlorobenzaldehyde and copper powder were purchased from the SRL Chemicals. PVDF was purchased from the Sigma-Aldrich. Heptaldehyde, para toluene sulphonic acid (p-TSA), chloroform (CHCl_3 99%), ethanol (99.8%) and HNO_3 were received from Avra Chemicals.

2.2 Synthesis of PETCH copolymer

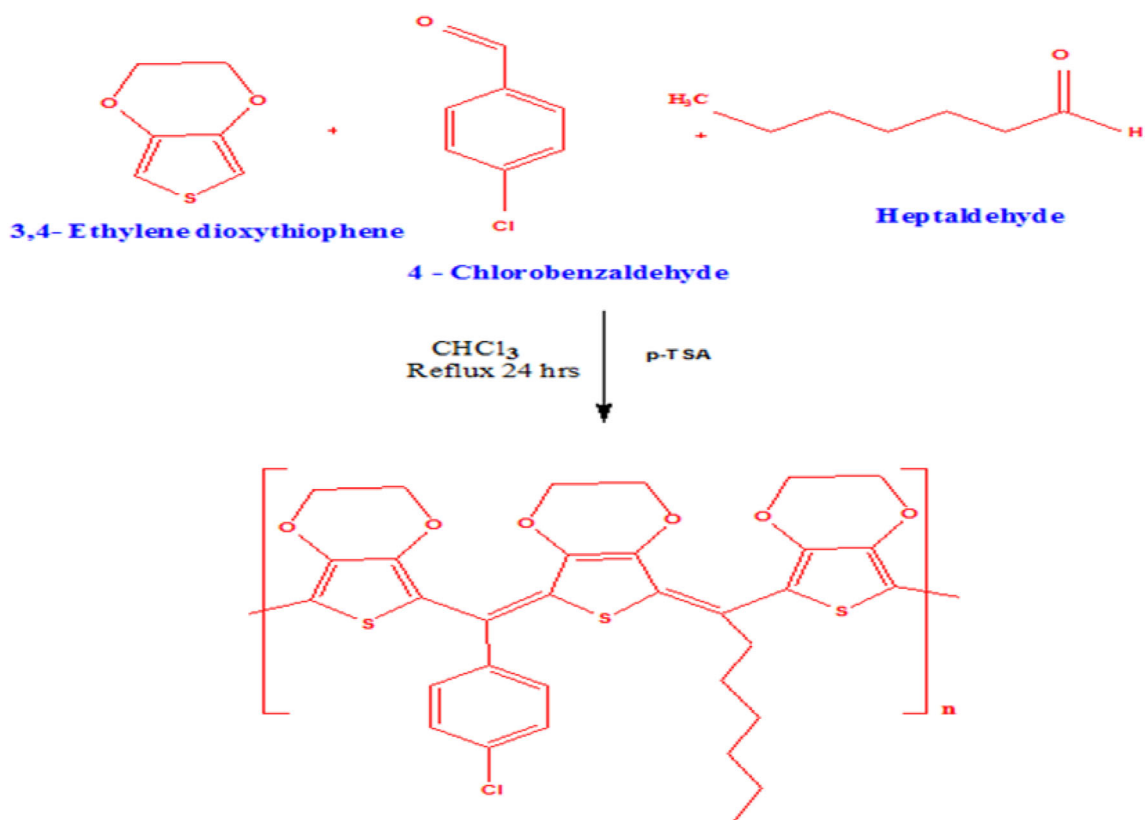
In a 100 ml round-bottom flask EDOT (0.01 mmol), 4-chloro benzaldehyde (0.01mmol) and heptaldehyde (0.01 mmol) are dissolved in chloroform solvent (20 ml) and then p-TSA (0.02 mmol) is added dropwise. The contents were refluxed for 24 h at 70°C in an N_2 atmosphere under magnetic stirring. After the specified time, the reaction mixture was filtered and then methanol was added to filtrate to precipitate the polymer as solid product, which was washed with water several times. The acquired product was dried out under a vacuum at 50°C for 12 h [42]. The synthesis of PETCH polymer is shown in scheme 1.

2.3 Synthesis of GNS

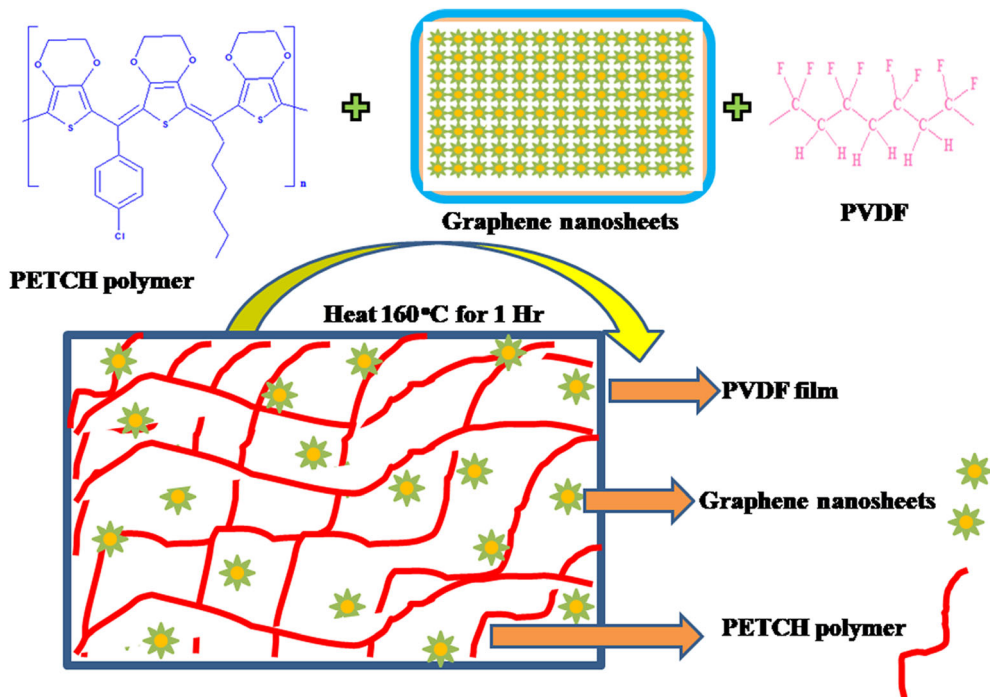
CHCl_3 (25 ml) and copper powder (10 g, 99.7% pure) are heated to 200°C for 10 h in a 100 ml Teflon-lined autoclave. After the specified time, the autoclave is cooled to RT, and the formed solid mass was separated by filtration and the filtrate is used for further experiments. And then, the obtained solid mass was treated with 6 M HNO_3 for 12 h at RT, and filtrated and the solid was washed with deionized water until the filtrate becomes chlorine free and attains neutral pH. The solid product was air-dried to obtain 1 g of the carbon product [43, 44].

2.4 Preparation of PETCH/PVDF/GNS nanocomposite film

The PETCH polymer was mixed with GNS powder in a solid state, and then PVDF in powder form has been ground with PETCH/GNS using mortar and pestle. Obtained mixture was placed in a temperature-controlled compression press and the mould was heated to 100°C , and a pressure of 1000 kg is applied to obtain 2 mm sheets of PETCH/PVDF/GNS nanocomposite. Similar procedure was followed by preparation of PVDF/PETCH/GNS (1, 3, 5%) with different percentages of composite sheets, as shown in scheme 2.



Scheme 1. Synthesis of PETCH polymer.



Scheme 2. Synthesis of PVDF/PETCH/GNS (1, 3, 5%) composites.

2.5 Measurements

FT-IR spectrum of PETCH and PVDF/PETCH/GNS composites was recorded in a Perkin Elmer (L160000A) equipment through the KBr pellet technique. $^1\text{H-NMR}$ spectrum of the prepared PETCH polymer was registered in a Bruker instrument using deuterated DMSO as solvent. Bruker D8 Advance, diffractometer was used to record the XRD patterns of GNS-dispersed composites within scan range of 5 to 90° of 2θ . The morphology of PVDF/PETCH/GNS (1, 3, 5%) composite films was studied using SEM of model TESCAN VEGA3 SBH. TG-DSC spectrum was recorded the instrument model Perkin Elmer and the temperature range 50 to 1300°C with heating rate 2 to $30^\circ\text{C min}^{-1}$. The electrical behaviour takes place over the material and was understood from the dielectric constant, dielectric loss, conductivity and Impedance values, which was studied in a Biologic SP 200 Potentiostat instrument.

3. Results and discussions

3.1 Fourier transform infrared studies

FTIR spectra of the (a) PETCH and (b) PVDF/PETCH/GNS (1, 3, 5%) nanocomposites are shown in figure 1. The peak (a) PETCH appears at 3410 cm^{-1} , C–H stretching modes of alkene. The peak appears at 3067 cm^{-1} , C–H stretching of alkane. The peaks appearing at 2950 to 2832 cm^{-1} are C–H

vibration of alkane. The peak appears at 2358 cm^{-1} band, this is due to the P–Q branch of CO_2 gas present in the spectrometer. The stretching modes of C=C in the thiophene ring exhibited IR absorption at 1500 cm^{-1} . The C–S bond stretching vibration of the thiophene ring was seen at 978 and 696 cm^{-1} [45]. The IR absorption peak that appears at 814 cm^{-1} is credited to C–Cl bond of 4-chlorobenzaldehyde. The peak appearing at 1438 cm^{-1} is accredited to the bending aliphatic of C–H in alkane for heptaldehyde, while the absorption band at 1359 cm^{-1} is owing to the C–H bending aliphatic group. After the functionalization of (b) PVDF/PETCH/GNS (1, 3, 5%), the vibrations at 1619 , 1373 cm^{-1} are ascribed to the C=C and C–C stretching vibrations of thiophene ring. Fascinatingly, the IR absorption peak at 3435 cm^{-1} is slightly shifted to 2917 cm^{-1} . Absorption of C=C group also exhibited lower absorption at 1619 cm^{-1} , and the C–Cl bond in 4-chlorobenzaldehyde showed its absorption at 764 cm^{-1} , these data confirm the successful formation of PVDF/PETCH/GNS (1, 3, 5%) polymer nanocomposites [46].

3.2 $^1\text{H-NMR}$ spectrum of PETCH

$^1\text{H-NMR}$ spectrum of PETCH is shown in figure 2, which reveals that the characteristic of the (d) aromatic protons of 4-chlorobenzene appeared at 7.19 ppm , (c) protons appeared at 4.51 and 4.35 ppm and the CH– protons of PEDOT. The chemical shifts of (b) protons appeared at

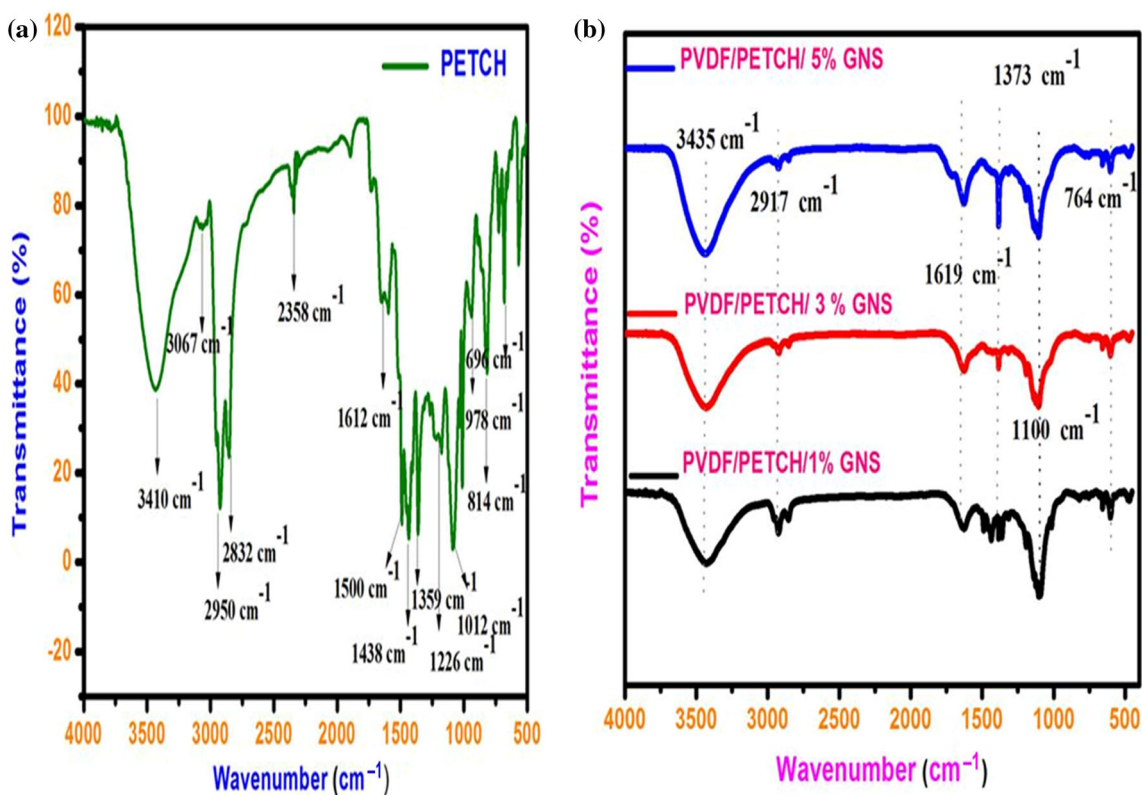


Figure 1. FTIR spectra of (a) PETCH and (b) PVDF/PETCH/GNS (1, 3, 5%) nanocomposites.

Signature SIF VIT VELLORE
ECH

```

Current Data Parameters
NAME      EXT41021
EXPNO    17
PROCNO   1

F2 - Acquisition Parameters
Date_    20211030
Time     10.03 h
INSTRUM spect
PROBHD   z108618_0505 (
PULPROG zg30
TD       65536

NS       32
DS       2
SWH      8012.820 Hz
FIDRES   0.244532 Hz
AQ       4.0894465 sec
RG       199.6
DM       62.400 usec
DE       6.50 usec
TE       0 K
D1       1.00000000 sec
TDO      1
SFO1     400.2604716 MHz
NUC1     1H
P1       14.00 usec
PLW1     16.00000000 W

F2 - Processing parameters
SI       65536
SF       400.2580099 MHz
WDW      EM
SSB      0
LB       0.30 Hz
GB       0
PC       1.00

```

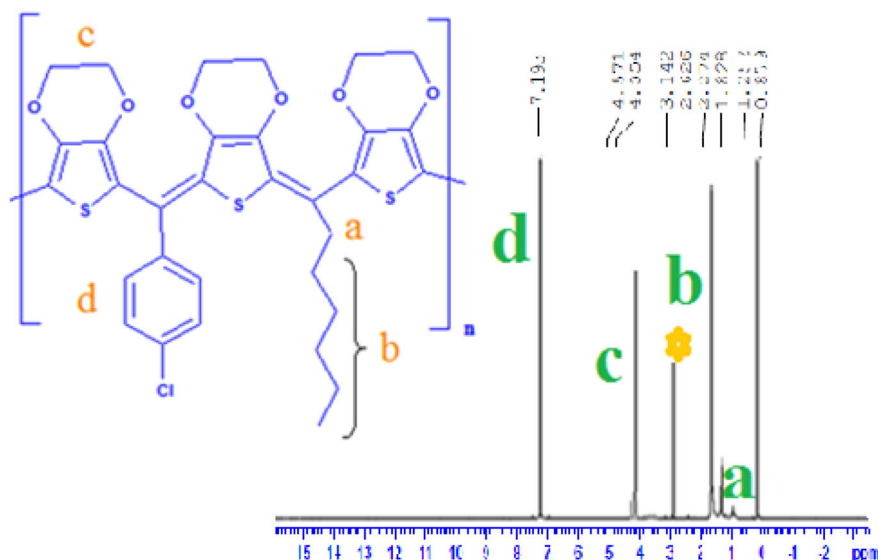


Figure 2. $^1\text{H-NMR}$ spectrum of polymer (PETCH).

1.51, 1.18, 0.82 ppm, and all the CH protons (a) of aliphatic chain appeared at 0.81 ppm. The chemical shift of DMSO solvent appeared at 2.8 ppm.

3.3 X-ray powder diffraction analysis

Figure 3 shows XRD patterns of PETCH, GNS and PVDF/PETCH/GNS (1, 3, 5%) composites in the range between 10 and 90°. The diffraction peaks appeared at 17.3°, 18.5°, 46.0°, 56.2° are assigned to the lattice planes of (100), (020), (110) and (002) respectively. As it is observed from the diffraction peak of (a) GNS which is centred at $2\theta = 26.7^\circ$ related to (002) plane that reveals the monolayer structure of GNSs. However, (b) PETCH polymer showed a broad peak at $2\theta = 20.3^\circ$ indicating the characteristic diffraction of amorphous materials, and this peak was found shifted to $2\theta = 21.1^\circ$, and diffraction of GNS is shifted to $2\theta = 28.9^\circ$ in the (c–e) PVDF/PETCH/GNS (1, 3, 5%) composite, due to the π - π stacking interaction between PETCH chains and GNS may be responsible for the peak shift in XRD pattern [47, 48]. The well-known diffraction peaks of PVDF are centred at $2\theta = 17.3^\circ, 18.5^\circ, 46.0^\circ, 56.2^\circ$, corresponding to (100), (020) planes. This suggests that PETCH, GNS and PVDF are mixed homogeneously without any phase separation to form PVDF/PETCH/GNS (1, 3, 5%).

3.4 Thermogravimetric analysis

Thermal properties of as-prepared materials (PVDF/PETCH/GNS (1, 3, 5%)) were analysed using thermogravimetric

analysis with the raising temperature (0 to 800°C). Figure 4 illustrates that the thermal stability of pristine PETCH was much lower than that of PVDF/PETCH/GNS (1, 3, 5%). The results demonstrated that the initial weight loss was observed at 100°C for neat PETCH and PVDF/PETCH/GNS (1, 3, 5%), it is due to the vaporization of moisture on the thin film surface. The neat PETCH shows the decomposition temperature 220°C obtained with minimum weight loss. The second stage weight loss occurred at 450 to 800°C corresponding to the decomposition of PETCH and about 60% weight loss was observed. The PVDF/PETCH/GNS (1, 3, 5%) shows the decomposition having 50 wt% at above a temperature of 480°C and the second stage weight loss occurred at around 520°C corresponding loss of PETCH in the host of PVDF/PETCH/GNS (1, 3, 5%) [49–51]. The nature of thermograms dictates that the unmodified PETCH polymer undergoes decomposition at a faster rate when compared to PETCH/PVDF blends due to higher thermal stability of fluorinated polymer, in addition, the PVDF/PETCH/GNS (1, 3, 5%) thin film exhibits a gradual weight loss and retains about 55% of the weight at higher temperatures, due to the presence of GNS [52, 53].

3.5 TG-differential scanning calorimetry

The differential scanning calorimetry was utilized to study the function of temperature with its physical state of PVDF/PETCH/1% GNS and PVDF/PETCH/5% GNS composites at the heating rate of $10^\circ\text{C min}^{-1}$ under a N_2 atmosphere.

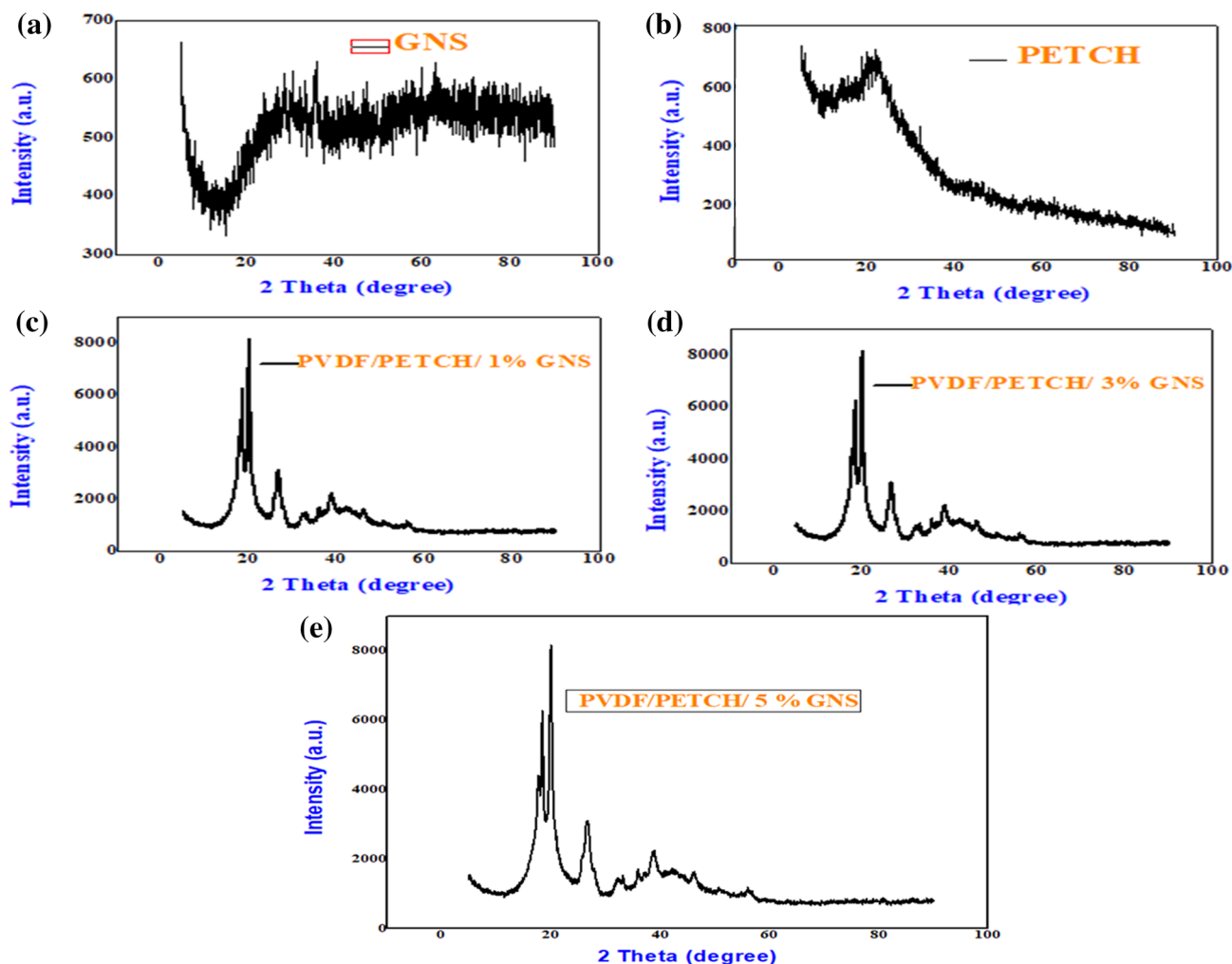


Figure 3. XRD spectra of neat (a) GNS, (b) PETCH and (c–e) PVDF/PETCH/GNS (1, 3, 5%) nanocomposites.

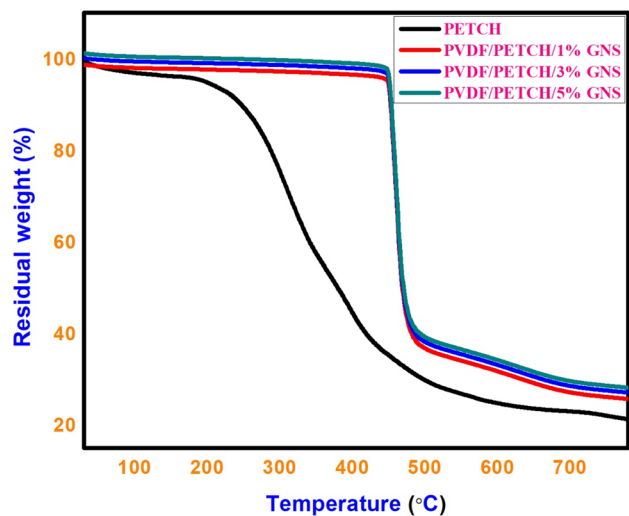


Figure 4. Thermogravimetric analysis spectrum of PVDF/PETCH/GNS (1, 3, 5%) films.

TG-DSC curve of PVDF/PETCH/1% GNS is shown in figure 5a. There are two obvious peaks appearing from

room temperature to 700°C. The exothermic peak appears at 130°C, and the weight loss (decomposition) of PVDF/PETCH/1% GNS started at the same temperature. Moreover, the endothermic peak was observed at around 470°C, at the end of the experiment, the remaining mass is about 12%. Figure 5b shows the TG-DSC curves of PVDF/PETCH/5% GNS composites, two endothermic peaks were observed at around 180 and 500°C. The observed endothermic peak at 500°C is caused by the melting of PVDF/PETCH/5% GNS composites, and the exothermic peak observed for PVDF/PETCH/5% GNS composites at 520°C may be due to the decomposition of polymer segments.

3.6 SEM analysis

The surface smoothness and structure of the polymers and nanocomposite are examined with SEM and shown in figure 6. The image figure 6a dictates the smooth surface morphology of PVDF and the sheet-like structure of GNSs is clearly observed in figure 6b. Figure 6c–f depicts the

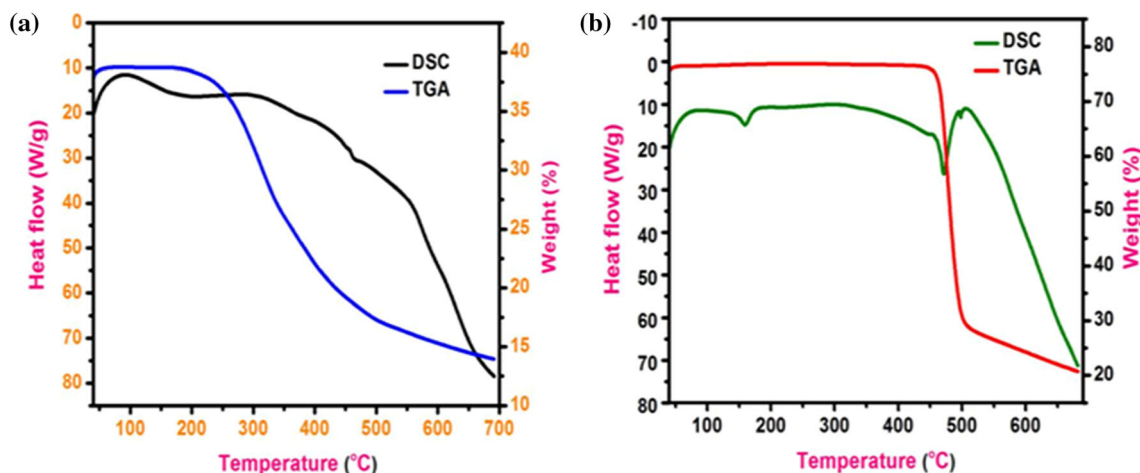


Figure 5. (a) TG-DSC of PVDF/PETCH/1% GNS and (b) PVDF/PETCH/5% GNS composites.

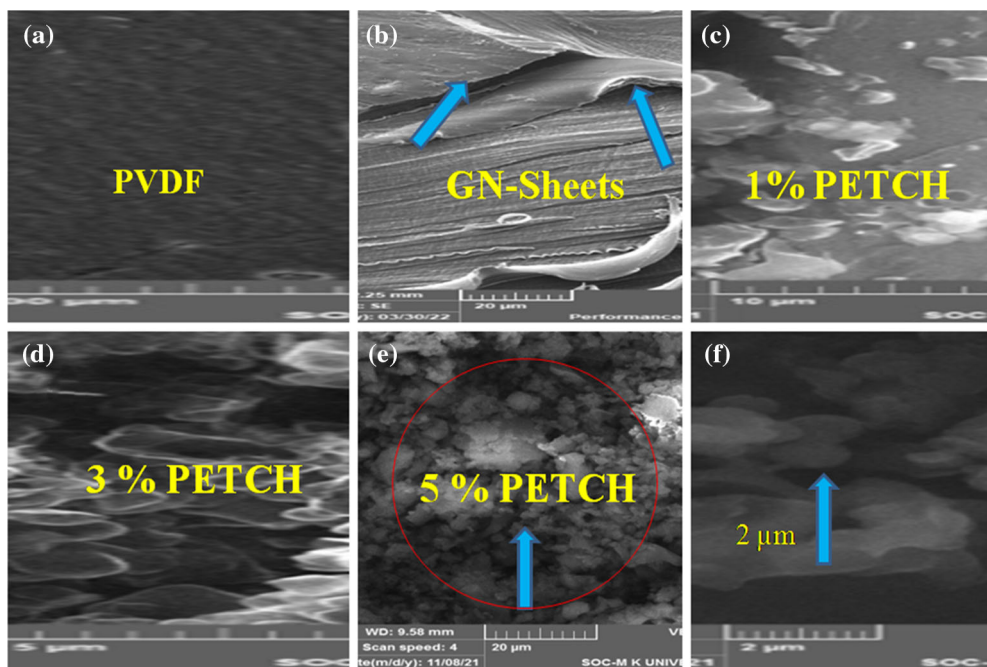


Figure 6. SEM images of (a) neat PVDF, (b) graphene nanosheets, (c) PVDF/PETCH/1% GNS nanocomposites, (d) PVDF/PETCH/3% GNS nanocomposites, (e) PVDF/PETCH/5% GNS nanocomposites and (f) PVDF/PETCH/5% GNS nanocomposites in μm.

morphology of PVDF/PETCH/GNS (1, 3, 5%) nanocomposites. It is observed from the SEM images that the sheet layers of graphene are wrapped by the polymer matrix and the morphology of PVDF/PETCH/GNS (1, 3, 5%) in the GNS indicates homogeneous blending of PVDF and PETCH without any phase separation in accordance with XRD results. The PETCH/GNS fractured surfaces present are smooth but irregular in appearance indicating good compatibility between the PVDF matrix and PETCH [54, 55]. The elemental analysis of the PVDF/PETCH/GNS composite was examined by EDX. Neat PETCH polymer result reported the presence of C, O, S and Cl with an atomic weight percentage of 51.05, 5.46, 30.19 and 13.30%

respectively. PVDF/PETCH/GNS (1, 3, 5%) polymer nanocomposites result reported the presence of C, F, O, Cl and S with an atomic weight percentage of 50.18, 44.32, 3.11, 1.20 and 1.19%, respectively. The EDX analysis clearly showed the synthesis of PETCH polymer and GNS formation on the surface of the PVDF matrix.

3.7 Dielectric properties

Polymer composites with appreciable dielectric constant and low dielectric loss are in demand in industrial applications due to their intrinsic properties, which include good

processing ability, high compression strength, relatively low equivalent series resistance and relatively low density, etc. [56–60].

The dielectric characteristics of the prepared PETCH/PVDF/GNS nanocomposites are evaluated and presented in figure 7.

3.7a Dielectric constant: The dielectric constant of the synthesized PVDF/PETCH/GNS (1, 3, 5%) nanocomposites is shown in figure 7a. It exhibits that the change in the dielectric constant with the applied frequency [61–64] and it is found that the dielectric constant decreases with respect to increase in frequency; however, it is increasing with respect to the addition of conductive nanostructures. The value of dielectric constant (k) of varying weight percentages of GNS-dispersed PETCH/PVDF composites are evaluated. The values of dielectric constant obtained at the frequency range 10 kHz to

1 MHz and the composite PVDF/PETCH/1% GNS showed a value of 1.9 at 1 MHz. This value is found to increase on increasing the concentration of the GNS nanofiller, for instance, when the concentration of GNS is increased to 3%, the value was raised to 3 at 1 MHz. This is due to the formation of a compatible homogeneously blended PETCH/PVDF matrix and the conductive network formation by the addition of GNS, with coherence at the interface.

As the loading of GNS is increased to 5%, there is further enhancement in the dielectric constant value to about 3.9 at 1 MHz, respectively. The value of the dielectric constant observed for neat PVDF matrix [65] is 0.9 at 1 MHz. The GNS-dispersed polymer composites showed higher dielectric constant than neat PVDF, which may be due to the uniform distribution and network of GNS filler within the PETCH/PVDF polymer, in addition to anticipated interfacial polarization mechanisms.

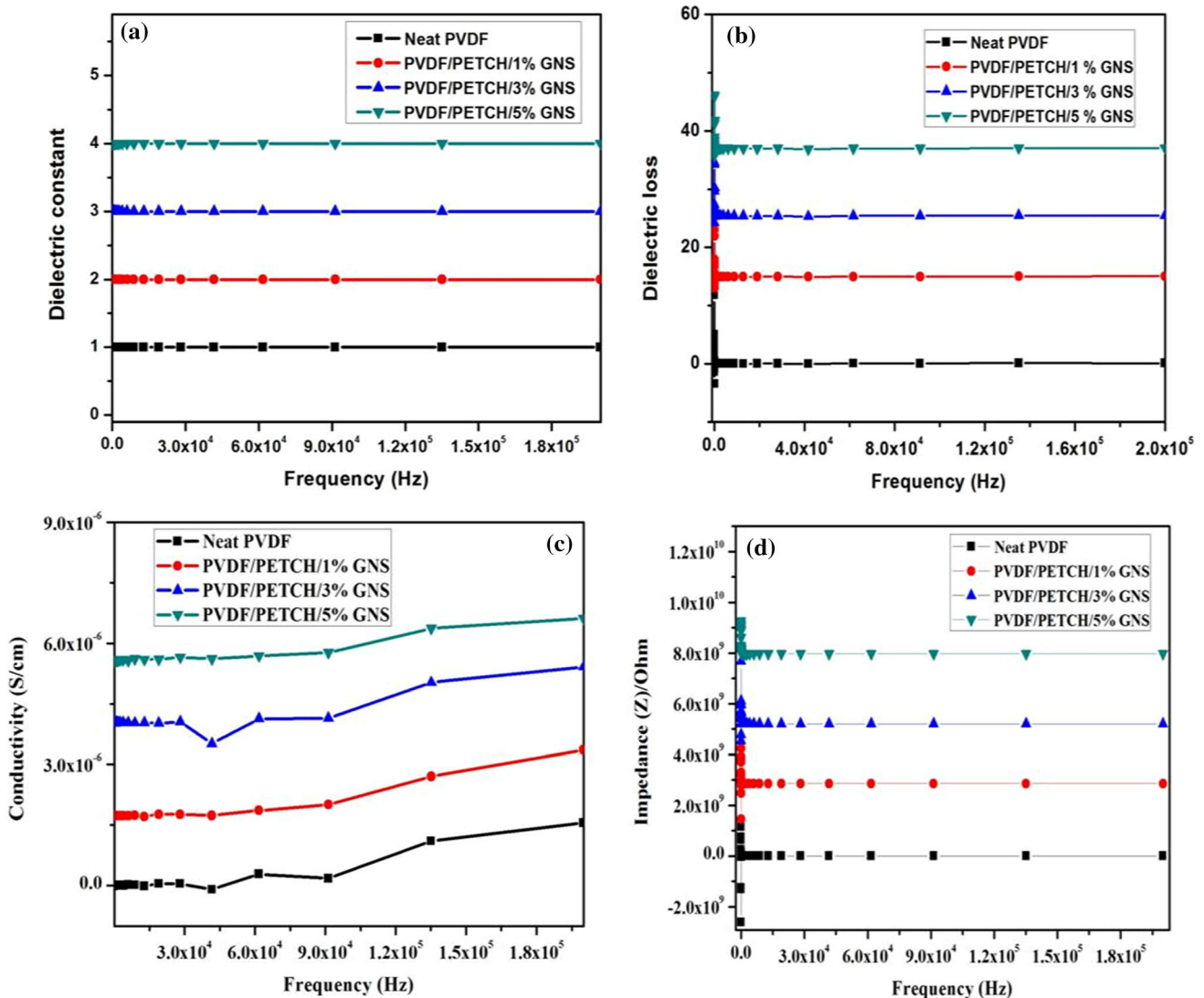


Figure 7. (a) Dielectric constant, (b) dielectric loss, (c) conductivity, (d) impedance with respect to frequency for 1, 3 and 5% PETCH with GNS reinforced in PVDF nanocomposites.

Table 1. Dielectric constant, dielectric loss and variation of conductivity with respect to frequency for PVDF/PETCH/GNS (1, 3, 5%) nanocomposites.

Samples	Dielectric constant at 1 MHz	Dielectric loss at 1 MHz	Conductivities at 1 MHz (S cm ⁻¹)	Impedance (Z Ohm ⁻¹)	References
Neat PVDF	0.9	12	0.1×10^{-6}	1.6×10^{-9}	[24,65,67]
PVDF/PETCH/1% GNS	1.9	23	2.2×10^{-6}	4.5×10^{xx}	[66, 67]
PVDF/PETCH/3% GNS	3	35	4.9×10^{-6}	7.9×10^{-9}	[66, 67]
PVDF/PETCH/5% GNS	3.9	48	5.8×10^{-6}	9.2×10^{-9} Z/Ohm	[66, 67]

Table 2. Comparison of PVDF/PETCH/GNS (1, 3, 5%) nanocomposites: dielectric constant, dielectric loss and variation of conductivity with respect the frequency to others.

Samples	Dielectric constant (MHz)	Dielectric loss (MHz)	Conductivity (S cm ⁻¹)	Impedance (Z Ohm ⁻¹)	References
3% Ag-MnO ₂ -PVDF	3.5×10^{-4}	32	1.1	3.3×10^5	[66]
3% Au-MnO ₂ -PVDF	1.0×10^{-9}	0.025	3.0×10^1	—	
5%PPy@Sep/PVDF	35.0	0.3	—	—	[67]
13% HNTs-PEDOT/PVDF	790.94	1.3	12.89	—	[68]
PVA/PEDOT:PSS/Ag NWs	—	—	3.82	—	[69]
PEDOT-PSS-CD25	—	—	1.03×10^{-2}	3.10×10^1	[70]
PVDF/PETCH/5% GNS	3.9	48	5.8×10^{-6}	9.2×10^{-9}	This work

3.7b Dielectric loss: The variation of dielectric loss value of the PVDF/PETCH/GNS (1, 3, 5%) nanocomposites with respect to change in frequency is studied and the results are publicized in the figure 7b. The dielectric loss for neat PVDF matrix is 12 at 1 MHz. The PVDF/PETCH/1% GNS dielectric loss value is 23 at 1 MHz. For the increase in the concentration of GNS to 3 and 5% into the PETCH and PVDF polymer, the value is found to be 35 and 48 at 1 MHz. The interfacial polarization is the only rationale behind the increases in the dielectric loss value. The interfacial polarization, conduction loss and migration of molecular dipoles are considered to be the three most important factors for the increases in dielectric loss values [66].

3.7c Conductivity: Figure 7c shows the conductivities of PVDF/PETCH/GNS (1, 3, 5%) nanocomposites. The conductivity value for neat PVDF is 0.1×10^{-6} S cm⁻¹ at 1 MHz. The PVDF/PETCH/1% GNS is 2.2×10^{-6} S cm⁻¹ at 1 MHz. The conductivity values slightly increase for PVDF/PETCH/3% GNS 4.9×10^{-6} S cm⁻¹ at 1 MHz. The reason is ascribed to the movement of electrons transition between the PETCH and GNS layers and also increases the conductivity of PVDF/PETCH/GNS (1%, 3%, 5%) nanocomposites. The conductivity values show much more enhancement for the incorporation of 5% GNS in polymer the value established to be 5.8×10^{-6} S cm⁻¹ at 1 MHz. The increased values of conductivity of PETCH, GNS in PVDF nanocomposites is due to the homogenous dispersion of composites. The establishment of the charge transfer

complex between the GNS and the polymer by further loading increases the conductivity, which is attained by the skipping of electrons crossways the interfaces and the chains in the polymer composites. This in turn enhances the electrical conductivity.

3.7d Impedance: Figure 7d shows the impedance spectrum of PETCH and GNS reinforced PVDF nanocomposites, the impedance value for neat PVDF is 1.6×10^{-9} Z Ohm⁻¹. The PVDF/PETCH/1% GNS showed 4.5×10^{-9} Z Ohm⁻¹ at 1 MHz. This value is found to increase on the concentration of the GNS nanofiller, i.e., when the concentration of GNS is increased to 3 and 5%, the impedance value is found to be 7.9×10^{-9} Z Ohm⁻¹ at 1 MHz and 9.2×10^{-9} Z Ohm⁻¹ at 1 MHz. This result clearly dictates that the creation of charge polarization at the interface within the PVDF/PETCH/5%GNS nanocomposites samples produces higher impedance values. The dielectric constant, dielectric loss and variation of conductivity with respect to frequency for PVDF/PETCH/GNS (1, 3, 5%) nanocomposites and comparison with other composites of dielectric properties are shown in tables 1 and 2.

4. Conclusions

We have successfully prepared graphene and PEDOT-based terpolymer-dispersed PVDF composites films through compression molding process and studied their conductive properties. FTIR spectral analysis confirmed the functional

groups present in the composites. X-ray diffraction pattern, SEM images and EDX analysis confirmed the presence of GNS in PETCH/PVDF composites at various percentages. The TGA of composites revealed that the incorporation of conjugated polymer and GNS substantially enhanced the thermal stability of PVDF. The incorporation of PETCH/GNS into PVDF composites enhanced the dielectric constant, dielectric loss, electrical conductivity and impedance of PVDF matrix. This study provided a PVDF composite material having promising thermal, morphological and dielectric properties, and that the composite may be applied in the high-tech fields such as gigahertz electronic systems, satellite broadcasting, defense and encapsulation of biomedical equipment.

Acknowledgements

We acknowledge the financial support of the Department of Science and Technology, Government of India, through Grant No. CRG/2019/002512.

References

- [1] Soares B G, Barra G M O and Indrusiak T J 2021 *Compos. Sci.* **5** 173
- [2] Pavel I A, Lakard S and Lakard B 2022 *Chemosensor* **10** 97
- [3] Ali A, Baheti V, Khan M Z, Ashraf M and Militky J 2019 *J. Text. Inst.* **111** 16
- [4] Prabha D R 2016 *Int. J. Chemtech. Res.* **9** 145
- [5] Wang Q, Xiao S, Shi S Q, Xu S and Cai L 2019 *Appl. Surf. Sci.* **475** 947
- [6] Liang C, Ruan K, Zhang Y and Gu J 2020 *ACS Appl. Mater. Interfaces* **12** 18023
- [7] Salit M S, Ishak M R and Aziz N A 2015 *Am. J. Appl. Sci.* **12** 64
- [8] Zhao B, Wang R, Li Y, Ren Y, Li X, Guo *et al* 2020 *J. Mater. Chem. C* **8** 7401
- [9] Pradhan S S, Unnikrishnan L and Mohanty S 2020 *J. Electron. Mater.* **49** 1749
- [10] Madhusudhan C K, Mahendra K, Madhukar B S and Somesh T E 2020 *Synth. Met.* **267** 116450
- [11] Enrico G, Jing S, Jiali Z and Tong Z 2019 *ACS Omega* **4** 20948
- [12] Raza A, Nasir A, Tahir M, Taimur S, Yasin T and Nadeem M 2020 *J. Appl. Polym. Sci.* **138** 49680
- [13] Rybicki T, Stempien Z and Karbownik I 2021 *Energies* **14** 7746
- [14] Trevino J E, Mohan S, Salinas A E, Cueva E and Lozano K 2021 *J. Appl. Polym. Sci.* **138** e50665
- [15] Li P, Du D, Guo L, Guo Y and Ouyang J 2016 *J. Mater. Chem. C* **4** 6525
- [16] Ruggiero E, Reboredo M M and Castro M S 2017 *J. Compos. Mater.* **0** 114
- [17] Tao M M, Liu F, Ma B R and Xue L X 2013 *Desalination* **316** 137
- [18] Rathi V, Panwar V and Prasad B 2020 *Prog. Electromagn. Res. Lett.* **88** 105
- [19] Gallantree H R 1983 *IEE Proc. I Solid State Electron. Devices UK* **130** 219
- [20] Zhang X, Wang J, Cao G S, Wei W Q, Liang Y Z, Guoet *et al* 2014 *ACS Appl. Mater. Interfaces* **6** 7471
- [21] Krishnamoorti R and Vaia R A 2007 *J. Polym. Sci. B Polym. Phys.* **45** 3252
- [22] Joo J and Lee C Y 2000 *J. Appl. Phys.* **88** 513
- [23] Kumar A, Singh K, Kumari A P, Dutta S, Dhawan P K S K and Dhar A 2014 *J. Mater. Chem.* **2** 16632
- [24] Kumaran R, Alagar M, Dinesh Kumar S, Subramanian V and Dinakaran K 2015 *Appl. Phys. Lett.* **107** 113107
- [25] Chen H L, Su C H, Ju S P, Chen H Y, Lin J S, Hsieh J Y *et al* 2017 *Mater. Res. Express* **4** 115025
- [26] Li C, Liu C, Shi L and Nie G 2015 *J. Mater. Sci.* **50** 1836
- [27] Wu L and Yang D 2019 *J. Nanosci. Nanotechnol.* **19** 3591
- [28] Hu D, Lu B, Duan X, Xu J, Zhang L, Zhang K *et al* 2014 *RSC Adv.* **4** 35597
- [29] Sanchez J A L, Capilla R P and Diez-Pascual A M 2018 *Polymers* **10** 1169
- [30] Diez-Pascual A M, Luceno-Sanchez J A, Pena-Capilla R and Garcia-Diaz P 2018 *Polymers* **10** 217
- [31] El Rhazi M, Majid S, Elbasri M, Ezzahra Salih F, Oularbi L and Lafdi K 2018 *Int. Nano Lett.* **8** 79
- [32] Vicente J, Costa P, Lanceros-Mendez S, Abete J M and Iturraspe A 2019 *Materials* **12** 3545
- [33] Li Y, Wang Y, Chen P, Xia R, Wu B and Qian J 2021 *Membranes* **11** 895
- [34] Tabhane G H, Giripunje S M and Kondawar S B 2021 *Synth. Met.* **279** 116845
- [35] Ahmed A, Jia Y, Huang Y, Khoso N A, Deb H, Fan Q *et al* 2019 *J. Mater. Sci.: Mater. Electron* **30** 14007
- [36] Ahmad H, Sharique A and Faiz M 2019 *Mater. Chem. Phys.* **239** 122324
- [37] Kausar A 2018 *Mater. Res. Innov.* **22** 302
- [38] Gebrekrsto A, Muzata T S and Ray S S 2022 *ACS Appl. Nano Mater.* **5** 7632
- [39] Ahmed I, Khan A N, Jan R and Gul I H 2022 *Mater. Res. Bull.* **148** 111687
- [40] Yanga R, Zhou Y, Ren Y, Xu D, Guan L, Guo X *et al* 2022 *J. Alloys Compd.* **908** 164538
- [41] Rani P, Ahamed M B and Deshmukh K 2021 *Synth. Met.* **282** 116923
- [42] Pangajam A, Chandramohan A, Dinakaran K, Harichandran G and Sureshkumar R 2021 *J. Solid State Electrochem.* **25** 2611
- [43] Sawant S Y, Somani R S, Cho M H and Bajaj H C 2015 *RSC Adv.* **5** 46589
- [44] Uma K, Kesava M, Elavarasan M, Thomas C K, Yang and Lin J H 2020 *J. Inorg. Organomet. Polym. Mater.* **30** 3797
- [45] Vinod Selvaganesh S, Mathiyarasu J, Phani K L N and Yegnaraman V 2007 *Nanoscale Res. Lett.* **2** 546
- [46] Ondo D A, Loyer F, Chemin J B, Bulou S, Choquet P and Boscher N D 2018 *Plasma Process Polym.* **15** e1700172
- [47] Tsonos C, Pandis C, Soin N, Sakellari D, Myrovali E, Kriptou S *et al* 2015 *Express Polym. Lett.* **9** 1104
- [48] Wang X, Xing W, Yu B, Feng X, Lei Song L and Hu Y 2013 *J. Mater. Chem. C* **1** 690
- [49] Khasim S, Pasha A, Badi N, Lakshmi M, Al-Ghamdi S A and Al-Aoh H A 2021 *J. Polym. Environ.* **29** 612
- [50] Zhang Q, Sha Z, Cui X, Qiu S, He C, Zhang J *et al* 2020 *Nanotechnol. Rev.* **9** 1350

- [51] Lee W, Kang Y H, Lee J Y, Jang K S and Cho S Y 2016 *RSC Adv.* **6** 53339
- [52] Qian G N, Wang L, Shang Y M, He X M, Tang S F, Liu M *et al* 2016 *Electrochim. Acta* **187** 113
- [53] Zhao Q, Jamal R, Zhang L, Wang M and Abdiryim T 2014 *Nanoscale Res. Lett.* **9** 557
- [54] Ren J, Ren R P and Lv Y K 2018 *Chem. Eng. J.* **349** 111
- [55] Chen Y, Cai K, Liu C, Song H and Yang X 2017 *Adv. Energy Mater.* **7** 1701247
- [56] Suematsu K, Arimura M, Uchiyama N, Saita S and Makino T 2016 *Compos. B Eng.* **104** 80
- [57] Atta S, Halder M, Chatterjee T, Karmakar R and Meikap A K 2022 *Mater. Chem. Phys.* **285** 126094
- [58] Yang D D, Xu H P, Wang J R and Wu Y J 2013 *Appl. Polym. Sci.* **130** 3746
- [59] Atta S, Halder M and Meikap A K 2021 *J. Mater. Sci.: Mater. Electron.* **32** 6992
- [60] Pecharroman C, Esteban-Betegon F, Bartolome J F, Lopez-Esteban S and Moya J S 2001 *Adv. Mater.* **13** 1541
- [61] Feng Y, Li W L, Hou Y F, Yu Y, Cao W P, Zhang T D *et al* 2013 *J. Name* **00** 1
- [62] Jiang Y, Zhang Z, Zhou Z, Yang H and Zhang Q 2019 *Polymers* **11** 1541
- [63] Yang D, Xu H and Yu W 2017 *J. Thermoplast. Compos. Mater.* **31** 1
- [64] Tiwari V and Srivastava G 2014 *J. Polym. Res.* **21** 587
- [65] Rengaswamy K, Sakthivel D K, Muthukaruppan A, Balasubramanian N, Venkatachalam S and Kannaiyan D 2018 *New J. Chem.* **42** 12945
- [66] Narayanasamy K, Sekar S S, Rajakumari R, Suresh Kumar R, Debmalaya Roy and Kannaiyan D 2020 *Int. J. Polym. Anal.* **26** 37
- [67] Chen S, Chen S, Qiao R, Xu H, Liu Z, Luo H *et al* 2021 *Compos. Part A. Appl. Sci.* **145** 106384
- [68] Wanga F, Zhanga X, Maa Y, Chena D and Yanga W 2018 *Appl. Surf. Sci.* **458** 924
- [69] Yu J, Gu W, Zhao H and Ji G 2021 *Sci. China Mater.* **64** 1723
- [70] Chin-Jung L and I-Shou T 2011 *Mater. Sci. Forum* **687** 625